

# Effect of the metallization and electrode size on the electrical admittance of piezoelectric ceramic parallelepipeds

Oumar Diallo<sup>1</sup>, Guy Feuillard<sup>2</sup>, Erling Ringgaard<sup>3</sup>, Emmanuel Leclézio<sup>4</sup>

<sup>1</sup> Université François Rabelais de Tours, Laboratoire GREMAN UMR CNRS 7347, 3 rue de la Chocolaterie BP 3410 41034 BLOIS CEDEX France

<sup>2</sup> École Nationale d'Ingénieurs du Val de Loire, Laboratoire GREMAN UMR CNRS 7347, 3 rue de la Chocolaterie BP 3410 41034 BLOIS CEDEX France.

<sup>3</sup> Meggitt Sensing Systems, Hejreskovvej 18A, DK-3490 Kvistgaard, Denmark

<sup>4</sup> Université Montpellier 2, Institut d'Electronique du Sud, UMR CNRS 5214, IES - MIRA case 082, Place Eugène Bataillon 34095 MONTPELLIER CEDEX 5 France

**Abstract.** This work deals with the determination of the effect of the sizes of electrodes in the electrical admittance spectra of parallelepiped piezoceramics. Recently we have developed a method of characterization using the modeling of the electrical admittance of electroded ceramic cubes. These electrodes covered completely the two faces perpendicular to the polarization axis. In this work the first electrode is unchanged but the size of the second electrode is varied. The size effect of the electrode on the electrical admittance curve of the sample is investigated. The chosen sizes are 1/25, 4/25, 9/25, 16/25 and 25/25 compared with the face of the sample, respectively. Depending on the size and location of the electrode, several modes can be generated or annihilated. In order to represent the frequency evolution of the admittance of piezoelectric ceramics, elastic loss and dielectric loss tensors are introduced.

## 1 Introduction:

The resonance ultrasound spectroscopy allows the complete set of elastic, piezoelectric and dielectric properties of materials to be identified using a single small sample. To be an efficient technique, all types of modes (transverse, longitudinal and torsional modes) have to be generated and detected. Thus, very often, generation is made by a wide band transducer situated on a corner of the cube while detection can be made by Laser interferometry. In the case of a piezoelectric ceramic, generation can be carried out by two electrodes. In this case, the size and the location of these electrodes will affect the frequency response of the cube. The purpose of this work is to examine these effects on the mechanical and electrical admittance spectra.

In a previous work the modelling of the electrical admittance was studied. This model takes into account two full electrodes on the two faces perpendicular to the polarisation axis. In this work this model is modified to calculate the admittance spectra of a cube with one full electrode and one rectangular partial electrode. The frequency shift of the first thickness resonance is investigated as a function of the electrode size. The influence of the mechanical and electrical losses on the admittance spectra is discussed. In addition to this analysis, experiments are made on piezoelectric ceramic cubes (a Ferroperm™ Pz27 ceramic manufactured by Meggitt Sensing Systems) with various electrode sizes. They confirm the theoretical results.

## 2 Theoretical approaches

### 2.1 Electrical admittance modelling

The electrical admittance of an electroded piezoceramic cube is given by [1], [2]:

$$Y = j\omega \sum_{\mu} \frac{Q_{\mu}^{(1)} Q_{\mu}^{(2)}}{\omega_{\mu}^2 - \omega^2} + j\omega \underline{C}^S \quad (1)$$

where  $Q_{\mu}^{(1)}$  and  $Q_{\mu}^{(2)}$  are the charge quantities on the surface of the electrode and  $\underline{C}^S$  is a term including both mechanical and electrical losses that lead to a real part for the admittance,  $\mu$  is the number of the mode and  $C^S$  is the clamped capacitance between the top and the bottom electrode.

$$C^S = \epsilon_{33}^S \frac{A}{2L_3} \quad (2)$$

To calculate the electrical admittance of a piezoelectric cube with one partial electrode, we determine at first the eigenfrequencies of the system, the clamped capacitance and the charge quantity in each case. The charge calculation expression is given by Holland in [2].

### 2.2 Calculation of the eigenfrequencies of the system

The eigenfrequencies and vibration modes of the parallelepiped are first identified thanks to the procedure proposed in [3]. The stationary points of system are sought by minimizing the Lagrangian of the system. The mechanical displacements,  $u$ , and the electrical potential,  $\phi$ , inside the sample are expressed through the Rayleigh-Ritz method as a linear combination of trial functions  $\psi_p$  and  $\phi_r$ . This leads to the following eigenvalue problem [3-6]

$$\begin{aligned} (\Gamma + (\Omega - A)(A - 2B)^{-1}(\Omega - A)^T)a &= \rho\omega^2 a, \\ b &= (A - 2B)^{-1}(\Omega - A)^T a. \end{aligned} \quad (3)$$

$\Gamma$ ,  $\Omega$ , and  $A$  are respectively elastic, piezoelectric and dielectric interaction matrices.  $A$  and  $B$  are the contributions of the work of the electrostatic forces,  $\rho$  is the density of the material,  $a$  and  $b$  are the eigenvectors of the system: they correspond to the Rayleigh-Ritz coefficients in the definitions of the mechanical displacement and electrical potential functions [3], [5].

### 2.3 Choice of the basis functions:

The mechanical basis functions defined by Demarest is still unchanged [6], [7]. For a piezoelectric cube with dimensions  $2L_1, 2L_2, 2L_3$ , these basis functions are expressed by:

$$\psi_p = \frac{1}{\sqrt{L_1 L_2 L_3}} P_{\xi} \left( \frac{x_1}{L_1} \right) P_{\mu} \left( \frac{x_2}{L_2} \right) P_{\nu} \left( \frac{x_3}{L_3} \right) \mathbf{e}_i \quad (4)$$

where  $P_{\xi} \left( \frac{x_1}{L_1} \right)$  is the Legendre polynomial and  $\mathbf{e}_i$  is a unit vector. The electrical basis function must take into account the metallization condition. It will be modified in order to put zero potential in the metallized parts. In other parts it will be defined like in Delaunay's study. The chosen basis function is expressed by:

$$\phi_r = \frac{1}{\sqrt{L_1 L_2 L_3}} P_{\xi} \left( \frac{x_1}{L_1} \right) P_{\zeta} \left( \frac{x_2}{L_2} \right) f_{\eta} \left( \frac{x_3}{L_3} \right) \quad (5)$$

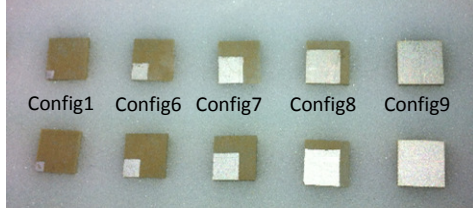
where

$$f_{\eta}^{\left(\frac{x_3}{L_3}\right)} = \begin{cases} (-1)^{\eta} \left(1 - \frac{x_3}{L_3}\right)^2 P_{\eta} \left(\frac{x_3}{L_3}\right) & \text{in metallized part} \\ (-1)^{\eta} \frac{1}{2} \left(1 + \frac{x_3}{L_3}\right) P_{\eta} \left(\frac{x_3}{L_3}\right) & \text{in other part} \end{cases} \quad (6)$$

### 3 Results and discussions

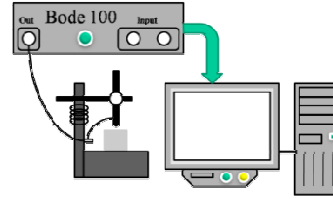
The theoretical admittances of a Pz27 piezoceramic has been calculated for various electrode sizes (Fig. 1) and compared to electrical admittance measurements. The properties used for theoretical calculations are:  $C_{11}^E=153$ ,  $C_{12}^E=108$ ,  $C_{13}^E=87$ ,  $C_{33}^E=111$ ,  $C_{44}^E=25$ ,  $C_{66}^E=22.5$  in GPa;  $e_{15}=9.6$ ,  $e_{31}=-2.96$ ,  $e_{33}=19.2$  in C/m<sup>2</sup>;  $\epsilon_{11}^S=1117$ ,  $\epsilon_{33}^S=911$  in  $\epsilon_0$ ;  $\delta_m=1.49\%$  and  $\delta_e=1.01\%$ .

#### 3.1 Experimental set-up and samples presentation



1a) Sample configurations

The electrodes are sizes are 1/25, 4/25, 9/25, 16/25 and 25/25 of the full electrode



1b) Experimental set-up

**Fig. 1.** Experimental photo of the samples with different size of electrodes and set-up.

Five samples with different electrode sizes were characterised (Fig 1a)). Electrical impedance and admittance of the sample were measured in the 100 kHz-250 kHz frequency range using an Omicron Bode analyser using a specific sample holder (Fig 1b)). They were transferred to a computer for comparison with theoretical admittances.

#### 3.2 Comparison of the different spectra

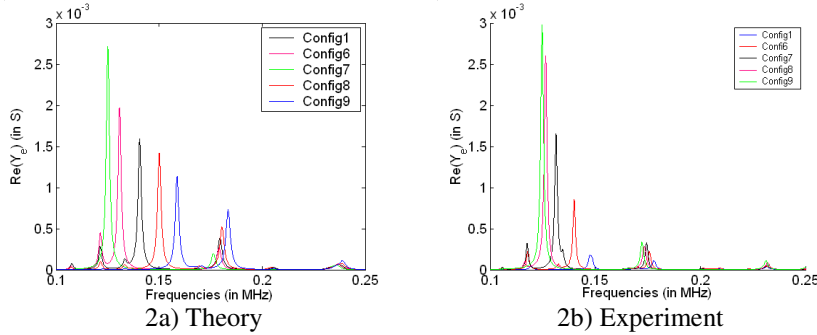


**Fig. 2.** Real part of the electrical admittance: 2a) theory and 2b) experiment.

Both in the theory and the experiment the number of excited mode depends on the electrode size. The configuration 1 exhibits ten resonances in the theory (nine in the experiment) while the configuration 9 exhibits only three resonances. In the first case, the excitation conditions are such that free vibrations of the cube are observed. For a fully electrodes sample on both faces, the strong symmetry is imposed by the electrodes and only thickness modes are generated.

Experimental and theoretical results show a shift of the first resonance mode toward the low frequency. Figure 3 shows the evolution of the first resonance mode versus the relative area of the

electrode. In the configuration 1 the resonance is located at 148 kHz in the experiment. In the configuration 9, this mode is located at 124.8 kHz.

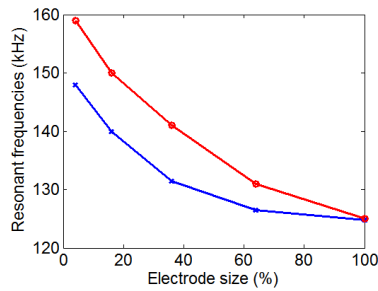


**Fig 3.** Evolution of the main resonant frequency versus the fractional electrode area.

In the first case, the electrical boundary conditions are close to metal free boundary conditions while in the full electrode sample, they correspond to metal-metal boundary conditions. In the configuration 9, the relative discrepancy between theoretical frequencies and experimental is less than 2.5 %. It is much bellow a 1% variation of the elastic constants.

**Table 1.** Theoretical and experimental resonant frequencies for the fully electroded sample

#Mode	#1	#2	#3
Theoretical frequency (kHz)	125.13	176.69	237.06
Experimental frequency (kHz)	124.8	172.3	231.2
Relative error (%)	0.26	2.48	2.47

## 4 Conclusion

In this work the effect of the electrode size was studied. Admittance measurements were carried out on five Pz27 ceramic samples with one full electrode on one side and one partial electrode of various sizes on the opposite side. The experimental results were compared to the theoretical ones obtained by a variational model. It is shown that the number of generated modes decreases as the electrode size increases and that the main resonance of the cube is shifted toward low frequency when the electrode size increases. The method presented here will be used to determine the tensorial properties of piezoelectric materials taking into account the effective losses.

## References

- [1] R. Holland and E. P. EerNisse, *IEEE Trans. Sonics Ultrason.*, **15**, 2,( Apr. 1968).
- [2] R. Holland, *The Journal of the Acoustical Society of America*, vol. **43**, no. 5, p. 988, 1968.
- [3] T. Delaunay, E. Le Clézio, M. Guennou, H. Dammak, M. P. Thi, and G. Feuillard, *IEEE trans. on ultras., ferroelectrics, and frequency control*, vol. **55**, no. 2, pp. 476–88, Feb. 2008.
- [4] B. Zadler, J. A. Scales, J. H. L. Le Rousseau, and M. L. Smith, pp. 1854–1857,(2002).
- [5] I. Ohno, *Phys. Chem. Minerals*, vol. **17**, pp. 371–378, (1990).
- [6] I. Ohno, *J. Phys. Earth*, vol. **24**, pp. 355–379, (1976).
- [7] H. H. Demarest, *Journal of the Acoust. Soc. of America*, vol. **49**, no. 3B, p. 768, (1971).